Supporting Information for

Alkali Metal/Mercury Dual-Metal Sulfides as Infrared Nonlinear Optical Materials with High Laser-induced Damage Thresholds

Guili Wang,[a,b,d] Bohui Xu,[c,d] Chunxiao Li,[a] Pifu gong,[c] Zheshuai Lin,[b,c,d] and Jiyong Yao[a,b,*]

a Beijing Center for Crystal Research and Development, Key Lab of Functional Crystals and Laser Technology, Technical Institute of Physics and Chemistry, Chinese Academy of Sciences, Beijing 100190, P. R. China.

b Center of Materials Science and Optoelectronics Engineering, University of Chinese Academy of Sciences, Beijing 100049, P. R. China.

c Functional Crystals Lab, Key Laboratory of Functional Crystals and Laser Technology, Technical Institute of Physics and Chemistry, Chinese Academy of Sciences, Beijing 100190, China.

d University of Chinese Academy of Sciences, Beijing 100049, PR China.

*Corresponding author:

Jiyong Yao; jyao@mail.ipc.ac.cn.

Table of Contents

Experimental Procedures

References

Experimental Procedures

1. Reagents Caution! Toxic HgS was used; safeguards should be taken. All starting materials, Ba(99%), RbCl (99.9%), CsI (99.9%), HgS (99%), Ge (99.999%), S (99.999%), Rb_2CO_3(99%), and Cs_2CO_3 (99%) were directly purchased from Aladdin Co., Ltd. without further purification. The binary compound GeS_2 was synthesized by heating the stoichiometric ratios of raw elements in flame-sealed quartz tubes at high temperatures. All manipulations were carried out in an argon-filled glovebox.

2. Synthesis For single crystal growth, raw materials ($Rb_2HgGe_3S_8$: RbCl:HgS:GeS_2=2:2:3; $Cs_2HgGe_3S_8$: Ba:HgS:GeS_2:CsI=3:3:1:4) were weighed, finely ground, and loaded into quartz tubes, these tubes were then flame-sealed under high vacuum at 10^{-3} Pa and placed in a programmable furnace. The furnace was gradually heated from room temperature (RT) to 1123 K for 20 h and kept at 1123 K for 48 h. Then it slowly cooled to 623 K at a rate of 3 K/h. Finally, the furnace was turned off and cooled down to RT naturally. In the end, we obtained light-yellow layered crystals of $Rb_2HgGe_3S_8$ and light-yellow blocky crystals of $Cs_2HgGe_3S_8$. These crystals are stable under atmospheric conditions for more than 6 months without weight loss and changes in color. For polycrystalline powder synthesis, the mixtures of raw materials ($Rb_2HgGe_3S_8$/$Cs_2HgGe_3S_8$: Rb_2CO_3/Cs_2CO_3:HgS:GeS_2:S=1:1:3:1) were ground and placed into quartz tubes. These tubes were heated to 823 K and kept for 72 h, then cooled to RT by switching off the furnace. The product was reground for testing.

3. Elemental analysis. Elemental analysis of the single crystals was carried out using a filed-emission Hitachi S-4300 scanning electron microscope (SEM) equipped with an OXFORD X-Max^N 80 energy dispersive X-ray spectroscope (EDS).

4. Single crystal structure determination. Two suitable single crystals of $Rb_2HgGe_3S_8$ and $Cs_2HgGe_3S_8$ were selected under an optical microscope for structure determination. Their X-ray diffraction data were collected at 296.15 K employing a Bruker D8 Quest diffractometer (Mo-K_α radiation, $\lambda = 0.71073$ Å) equipped with a CCD area detector. Their structures were solved with the SHELXT structure solution program using intrinsic phasing and refined with the SHELXL refinement package using least squares minimisation.[1]

5. Powder X-ray diffraction (PXRD). The polycrystalline powder was reground with an agate mortar for PXRD data collection using a Bruker D8 Advance diffractometer equipped with Cu-K_α (λ = 1.5418 Å) radiation. The collection range is from 10° to 70° with a scan speed of 0.05 s and a scan step width of 0.02°. The simulated pattern was generated by Mercury software.[2]

6. Optical characterizations. The UV−vis−NIR diffuse reflectance spectra of $Rb_2HgGe_3S_8$ and $Cs_2HgGe_3S_8$ were measured in the wavelength range of 200−2500 nm by an Agilent Carry 7000 spectrophotometer equipped with an integrating sphere at RT and a polytetrafluoroethylene sample as standard material. The absorption values were calculated from the reflectance data via the Kubelka-Munk function.[3] The Raman spectra of $Rb_2HgGe_3S_8$ and $Cs_2HgGe_3S_8$ were measured by a Lab RAM Aramis spectrometer equipped with a 532 nm laser in the range of 100−500 cm^{-1} at RT.

7. Powder SHG test. Since $Rb_2HgGe_3S_8$ and $Cs_2HgGe_3S_8$ belong to the non-centrosymmetric (NCS) space group, their SHG intensities were evaluated through the Kurtz-Perry method[4] employing a 2090 nm fundamental laser. The polycrystalline powder was ground and filtered into samples with five particle sizes (20−50, 50−90, 90−125, 125−150 and 150−200 μm). AGS crystals were also ground into the same range and served as the benchmark for the measurements.

8. Powder LIDT measurement. The powder LIDTs of $Rb_2HgGe_3S_8$ and $Cs_2HgGe_3S_8$ (150–200 μm) were measured according to the single-pulse method[5] using a 1064 nm laser source with a pulse width τ_p of 5 ns and a repetition frequency of 1 Hz, and AGS of the same particle size were used as standard samples. When the laser energy reached 0.22, 0.19, and 0.07 mJ, respectively, the visible damage spots of $Rb_2HgGe_3S_8$, $Cs_2HgGe_3S_8$, and AGS can be observed under an optical microscope. Next, the $Rb_2HgGe_3S_8$, $Cs_2HgGe_3S_8$, and AGS can be obtained using the following formula: LIDT = $E/S\tau_p$, E represents the laser beam power and S represents the damage spot area.

9. Theoretical calculation. Based on density functional theory (DFT), the CASTEP package was used to calculate the properties of $Rb_2HgGe_3S_8$ and $Cs_2HgGe_3S_8$ at the atomic level.[6] The fine calculation quality was adopted. The exchange-correlation functionals was chosen to be the CA-PZ function, which operates within the context of the local density approximation (LDA). The interactions between valence electrons and ions were described using ultrasoft pseudopotentials

(USP) by treating Rb $4s^24p^65s^1$, Cs $5s^25p^66s^1$, Hg $5d^{10}6s^2$, Ge $4s^24p^2$, and S $3s^23p^4$ electrons as valence electrons, respectively. A dense Monkhorst-Pack k-point grid of 3 × 2 × 1 in the Brillouin zone was chosen. The plane-wave cutoff energy in the calculations was set to 285 eV. The properties of the title compound were calculated after geometric optimization to bring the model to the convergence criterion. 0.94 and 1.08 eV (the difference between the experimental bandgap and the computed bandgap) were set as the scissor operator in the computation of optical properties employing the scissors-corrected LDA method. Subsequently, the refractive index and second-order nonlinear tensor d_{ij} were calculated based on the Kramers-Kronics transform and Kleiman's symmetry, respectively.

Table S1. Crystallographic data and structure refinement for $Rb_2HgGe_3S_8$ and $Cs_2HgGe_3S_8$.

CCDC number	2405449	2405450
Empirical formula	$Rb_2HgGe_3S_8$	$Cs_2HgGe_3S_8$
Formula Weight	845.78	940.66
Crystal System	Orthorhombic	
Space Group	$P2_12_12_1$ (19)	
Temperature (K)	296.15	
a (Å)	7.3225(14)	7.4106(3)
b (Å)	12.108(3)	12.4313(6)
c (Å)	16.863(3)	17.0924(7)
α (°)	90	
β (°)	90	
γ (°)	90	
Volume (Å^3)	1495.0(5)	1574.61(12)
Z	4	4
ρ_{calc} (g/cm^3)	3.758	3.968
μ (mm^{-1})	23.758	20.972
F(000)	1512	1656
Radiation	Mo K_α (λ = 0.71073 Å)	
2θ range for data collection/°	4.83 to 50.11	4.05 to 50.07
Index ranges	$-8 \leq h \leq 8$, $-14 \leq k \leq 12$, $-20 \leq l \leq 16$	$-8 \leq h \leq 8$, $-14 \leq k \leq 14$, $-19 \leq l \leq 20$
Reflections collected	11963	23973
Independent reflections	2635[R_{int} = 0.0842, R_{sigma} = 0.0918]	2780[R_{int} = 0.0877, R_{sigma} = 0.0532]
Data/restraints/parameters	2635/0/128	2780/0/128
Goodness-of-fit on F^2	1.060	1.052
Final R indexes [$I > 2\sigma(I)$]	R_1 = 0.0570, wR_2 = 0.1096	R_1 = 0.0376, wR_2 = 0.0830
Final R indexes [all data]	R_1 = 0.0931, wR_2 = 0.1185	R_1 = 0.0516, wR_2 = 0.0877
Largest diff.peak/hole (e Å^{-3})	1.53/−1.83	1.35/−1.18
Flack parameter	0.46(3)	0.490(14)

$^a R_1 = \Sigma||F_o| - |F_c||/\Sigma|F_o|$, $wR_2 = [\Sigma w(F_o^2 - F_c^2)^2/\Sigma wF_o^4]^{1/2}$ for $F_o^2 > 2\sigma(F_o^2)$.

Table S2. *Wyckoff* site, fractional atomic coordinates, and equivalent isotropic displacement parameters U_{eq} (Å^2) of $Rb_2HgGe_3S_8$ and $Cs_2HgGe_3S_8$.

Atom	***Wyckoff* site**	***x***	***y***	***z***	$U_{\mathrm{eq}}{}^{a}$
			$Rb_2HgGe_3S_8$		
Rb1	4*a*	0.7373(4)	0.6945(3)	0.15589(19)	0.0522(8)
Rb2	4*a*	0.2471(5)	0.8687(3)	0.44851(18)	0.0474(9)
Hg1	4*a*	0.97096(13)	0.49995(11)	0.34716(7)	0.0383(4)
Ge1	4*a*	0.4748(3)	0.5287(2)	0.34560(17)	0.0214(6)
Ge2	4*a*	0.2655(4)	0.5495(3)	0.67524(14)	0.0251(7)
Ge3	4*a*	0.2379(4)	0.4388(3)	0.51608(15)	0.0252(7)
S1	4*a*	0.7142(8)	0.6345(6)	0.3503(5)	0.0329(17)
S2	4*a*	0.2860(11)	0.3720(7)	0.6380(4)	0.0335(19)
S3	4*a*	0.5057(10)	0.6205(7)	0.7263(5)	0.036(2)
S4	4*a*	0.0018(9)	0.5815(7)	0.7375(4)	0.032(2)
S5	4*a*	0.2274(12)	0.6169(6)	0.5525(4)	0.0306(18)
S6	4*a*	-0.0160(11)	0.3760(7)	0.4678(5)	0.037(2)
S7	4*a*	0.2356(9)	0.6343(6)	0.3429(4)	0.0308(16)
S8	4*a*	0.4854(10)	0.4047(7)	0.4455(4)	0.035(2)
			$Cs_2HgGe_3S_8$		
Cs1	4*a*	0.24880(16)	0.86952(9)	0.94667(6)	0.0317(3)
Cs2	4*a*	0.73716(16)	0.69117(9)	0.65183(6)	0.0360(3)
Hg1	4*a*	-0.03001(9)	0.50236(7)	0.84775(4)	0.0335(2)
Ge1	4*a*	0.4724(2)	0.52780(13)	0.84608(9)	0.0170(4)
Ge2	4*a*	0.2620(3)	0.55649(14)	0.51697(8)	0.0183(4)
Ge3	4*a*	0.2333(2)	0.45221(14)	0.67713(8)	0.0193(4)
S1	4*a*	0.2362(5)	0.6304(3)	0.8435(2)	0.0250(9)
S2	4*a*	0.2678(6)	0.3829(3)	0.5552(2)	0.0224(9)
S3	4*a*	0.0123(5)	0.5895(4)	0.4483(2)	0.0226(10)
S4	4*a*	0.5112(6)	0.6177(4)	0.4683(2)	0.0259(10)
S5	4*a*	0.2175(6)	0.6250(4)	0.6371(2)	0.0264(10)
S6	4*a*	0.4920(6)	0.4194(4)	0.7394(2)	0.0244(11)
S7	4*a*	0.7103(5)	0.6302(3)	0.8498(2)	0.0231(9)
S8	4*a*	-0.0049(6)	0.3837(4)	0.7292(2)	0.0305(12)

$^{a}U_{\mathrm{eq}}$ is defined as one-third of the trace of the orthogonalized U_{ij} tensor.

Table S3. Calculated bond valence sums (BVS) of $Rb_2HgGe_3S_8$ and $Cs_2HgGe_3S_8$.[a]

site	BVS	site	BVS
	$Rb_2HgGe_3S_8$		
Rb1	0.956	S2	−2.039
Rb2	1.170	S3	−2.109
Hg1	2.287	S4	−2.016
Ge1	4.036	S5	−2.217
Ge2	4.059	S6	−1.955
Ge3	4.049	S7	−1.911
S1	−2.157	S8	−2.085
	$Cs_2HgGe_3S_8$		
Cs1	1.215	S2	−2.129
Cs2	0.978	S3	−2.036
Hg1	2.236	S4	−1.977
Ge1	3.975	S5	−2.001
Ge2	3.947	S6	−2.044
Ge3	3.918	S7	−1.924
S1	−1.903	S8	−2.056

[a]The bond valence sums (BVS) of $Rb_2HgGe_3S_8$ and $Cs_2HgGe_3S_8$ were calculated by bond-valence parameters method through the following empirical expression[7]:

$$\sum_j v_{ij} = V_i$$

$$v_{ij} = exp[(R_{ij} - d_{ij})/b]$$

Where v_{ij} is the valence of a bond between two atoms i and j, V_i is the sum of all the valences from a given atom i, R_{ij} is the bond valence parameter, d_{ij} is actual length and b is commonly taken to be a universal constant equal to 0.37 Å.

Table S4. Selected bond lengths (Å) for $Rb_2HgGe_3S_8$ and $Cs_2HgGe_3S_8$.

Atom−Atom	**Length(Å)**	**Atom−Atom**	**Length(Å)**
$Rb_2HgGe_3S_8$			
Rb1–S1	3.362(8)	Hg1–S1	2.488(7)
Rb1–S2$^{\#4}$	3.594(9)	Hg1–S3$^{\#4}$	2.512(8)
Rb1–S2$^{\#5}$	3.928(9)	Hg1–S6$^{\#8}$	2.530(8)
Rb1–S3$^{\#6}$	3.581(9)	Hg1–S7$^{\#8}$	2.531(7)
Rb1–S4$^{\#6}$	3.683(9)	Ge1–S1	2.173(7)
Rb1–S6$^{\#3}$	3.653(9)	Ge1–S4$^{\#5}$	2.266(8)
Rb1–S6$^{\#5}$	3.662(8)	Ge1–S7	2.169(7)
Rb1–S8$^{\#3}$	3.473(9)	Ge1–S8	2.258(8)
Rb2–S1$^{\#7}$	3.402(8)	Ge2–S2	2.244(9)
Rb2–S3$^{\#7}$	3.440(8)	Ge2–S3	2.139(8)
Rb2–S4$^{\#6}$	3.698(8)	Ge2–S4	2.232(7)
Rb2–S5	3.520(8)	Ge2–S5	2.242(7)
Rb2–S5$^{\#6}$	3.521(9)	Ge3–S2	2.238(7)
Rb2–S5$^{\#7}$	3.810(9)	Ge3–S5	2.243(8)
Rb2–S6$^{\#6}$	3.815(9)	Ge3–S6	2.167(8)
Rb2–S7	3.352(8)	Ge3–S8	2.207(8)
Rb2–S8$^{\#7}$	3.795(9)		
$Cs_2HgGe_3S_8$			
Cs1–S1	3.458(4)	Cs2–S8$^{\#4}$	3.715(5)
Cs1–S2$^{\#4}$	3.586(5)	Hg1–S1	2.536(4)
Cs1–S2$^{\#3}$	3.832(5)	Hg1–S4$^{\#5}$	2.548(5)
Cs1–S2$^{\#5}$	3.646(4)	Hg1–S7$^{\#8}$	2.497(4)
Cs1–S3$^{\#3}$	3.800(5)	Hg1–S8	2.514(5)
Cs1–S4$^{\#4}$	3.846(5)	Ge1–S1	2.166(4)
Cs1–S6$^{\#4}$	3.767(4)	Ge1–S3$^{\#5}$	2.278(5)
Cs1–S7$^{\#2}$	3.490(4)	Ge1–S6	2.272(4)
Cs1–S8$^{\#3}$	3.511(4)	Ge1–S7	2.176(4)
Cs2–S3$^{\#6}$	3.625(5)	Ge2–S2	2.255(5)
Cs2–S4$^{\#6}$	3.740(5)	Ge2–S3	2.230(4)
Cs2–S4	3.671(4)	Ge2–S4	2.163(5)
Cs2–S5$^{\#7}$	3.662(5)	Ge2–S5	2.247(4)
Cs2–S5	3.946(5)	Ge3–S2	2.270(4)
Cs2–S6	4.118(5)	Ge3–S5	2.257(5)
Cs2–S6$^{\#4}$	3.793(5)	Ge3–S6	2.230(4)
Cs2–S7	3.473(4)	Ge3–S8	2.153(5)

Table S5. Selected bond angles (°) for $Rb_2HgGe_3S_8$ and $Cs_2HgGe_3S_8$.

Atom−Atom−Atom	Angle (°)	Atom−Atom−Atom	Angle (°)
$Rb_2HgGe_3S_8$			
S1–Hg1–S3$^{\#5}$	116.7(3)	S3–Ge2–S2	116.3(3)
S1–Hg1–S6$^{\#9}$	113.6(3)	S3–Ge2–S4	116.9(3)
S1–Hg1–S7$^{\#9}$	99.1(2)	S3–Ge2–S5	109.1(3)
S3$^{\#5}$–Hg1–S6$^{\#9}$	107.8(2)	S4–Ge2–S2	110.8(3)
S3$^{\#5}$–Hg1–S7$^{\#9}$	107.3(2)	S4–Ge2–S5	105.3(3)
S6$^{\#9}$–Hg1–S7$^{\#9}$	112.0(2)	S5–Ge2–S2	95.7(3)
S1–Ge1–S4$^{\#4}$	108.4(3)	S2–Ge3–S5	95.8(3)
S1–Ge1–S8	109.7(3)	S6–Ge3–S2	110.7(3)
S7–Ge1–S1	107.7(3)	S6–Ge3–S5	114.3(3)
S7–Ge1–S4$^{\#4}$	113.0(3)	S6–Ge3–S8	115.9(3)
S7–Ge1–S8	115.8(3)	S8–Ge3–S2	107.4(3)
S8–Ge1–S4$^{\#4}$	101.9(3)	S8–Ge3–S5	110.8(3)
$Cs_2HgGe_3S_8$			
S1–Hg1–S4$^{\#5}$	110.39(13)	S3–Ge2–S2	110.12(17)
S7$^{\#9}$–Hg1–S1	101.57(13)	S3–Ge2–S5	106.81(17)
S7$^{\#9}$–Hg1–S4$^{\#5}$	113.80(14)	S4–Ge2–S2	115.57(18)
S7$^{\#9}$–Hg1–S8	116.24(14)	S4–Ge2–S3	116.20(17)
S8–Hg1–S1	106.71(14)	S4–Ge2–S5	110.08(19)
S8–Hg1–S4$^{\#5}$	107.72(15)	S5–Ge2–S2	95.80(15)
S1–Ge1–S3$^{\#5}$	115.65(16)	S5–Ge3–S2	95.10(15)
S1–Ge1–S6	112.61(16)	S6–Ge3–S2	105.79(17)
S1–Ge1–S7	108.09(17)	S6–Ge3–S5	111.32(18)
S6–Ge1–S3$^{\#5}$	103.45(16)	S8–Ge3–S2	108.74(18)
S7–Ge1–S3$^{\#5}$	108.16(16)	S8–Ge3–S5	117.3(2)
S7–Ge1–S6	108.60(17)	S8–Ge3–S6	115.80(17)

Symmetry codes:

$Rb_2HgGe_3S_8$: #1: 1-x, -0.5+y, 0.5-z; #2: 2-x, 0.5+y, 0.5-z; #3: 1-x, 0.5+y, 0.5-z; #4: 0.5-x, 1-y, -0.5+z; #5: 1.5-x, 1-y, -0.5+z; #6: 0.5+x, 1.5-y, 1-z; #7: -0.5+x, 1.5-y, 1-z; #8: 2-x, -0.5+y, 0.5-z; #9: 1+x, +y, +z; #10: 1.5-x, 1-y, 0.5+z; #11: 0.5-x, 1-y, 0.5+z; #12: -1+x, +y, +z;

$Cs_2HgGe_3S_8$: #1: 0.5+x, 1.5-y, 2-z; #2: -0.5+x, 1.5-y, 2-z; #3: -x, 0.5+y, 1.5-z; #4: 1-x, 0.5+y, 1.5-z; #5: 0.5-x, 1-y, 0.5+z; #6: 1-x, -0.5+y, 1.5-z; #7: 0.5+x, 1.5-y, 1-z; #8: 1+x, +y, +z; #9: -1+x, +y, +z; #10: -0.5+x, 1.5-y, 1-z; #11: -x, -0.5+y, 1.5-z; #12: 0.5-x, 1-y, -0.5+z;

Table S6. The powder LIDTs of $Rb_2HgGe_3S_8$ and $Cs_2HgGe_3S_8$.

Compound	**Damage energy (mJ)**	**Spot diameter (mm)**	**Spot area (cm^2)**	**τ_p (ns)**	**LIDT (MW cm^{-2})**	**Relative value**
$Rb_2HgGe_3S_8$	0.68	0.4	0.0012566	5	108.23	3.1
$Cs_2HgGe_3S_8$	0.59	0.4	0.0012566	5	93.95	2.7
$AgGaS_2$	0.22	0.4	0.0012566	5	35.01	1

Table S7. The calculated distortion degree for all tetrahedrons within $Rb_2HgGe_3S_8$ and $Cs_2HgGe_3S_8$.[a]

Atom	Atom	Bond length	Distortion degree	Atom	Atom	Bond length	Distortion degree
$Rb_2HgGe_3S_8$				**$Cs_2HgGe_3S_8$**			
Hg1	S1	2.488	0.00606	Hg1	S1	2.536	0.00723
	S3	2.512			S4	2.548	
	S6	2.530			S7	2.497	
	S7	2.531			S8	2.514	
Ge1	S1	2.173	0.02053	Ge1	S1	2.166	0.02339
	S4	2.266			S3	2.278	
	S7	2.169			S6	2.272	
	S8	2.258			S7	2.176	
Ge2	S2	2.244	0.01699	Ge2	S2	2.255	0.01366
	S3	2.139			S3	2.230	
	S4	2.232			S4	2.163	
	S5	2.242			S5	2.247	
Ge3	S2	2.238	0.01208	Ge3	S2	2.270	0.01672
	S5	2.243			S5	2.257	
	S6	2.167			S6	2.230	
	S8	2.207			S8	2.153	

[a] For a tetrahedral $[MX_4]$, the distortion degree can be determined by the following modified calculation equation:

$$\Delta d = \left(\frac{1}{4}\right)\sum\left[\left|\frac{d_i - d}{d}\right|\right]$$

, where d_i represents the length of four individual M−X bonds and d is the average length of the four bonds.[8]

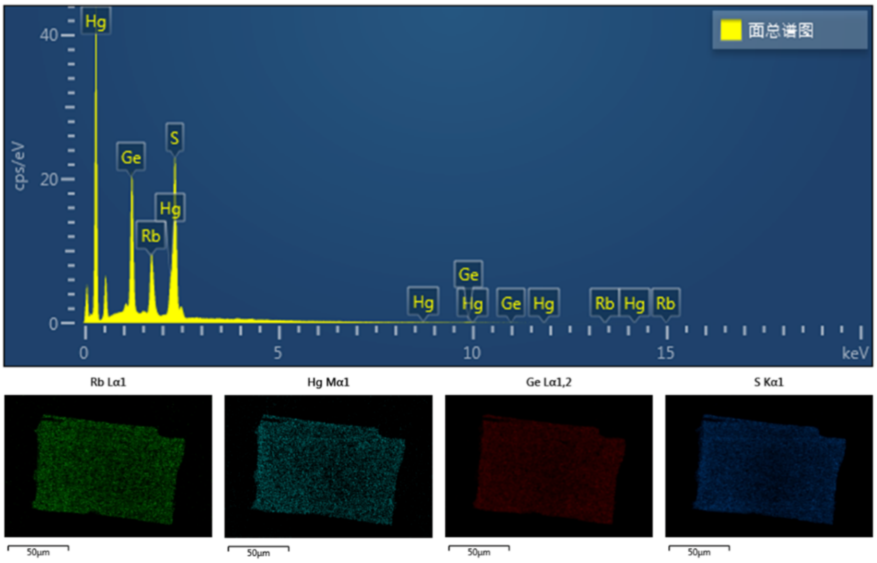

Element	Atomic percentage/%
Rb	13.71
Hg	7.27
Ge	24.82
S	54.20
Total	100

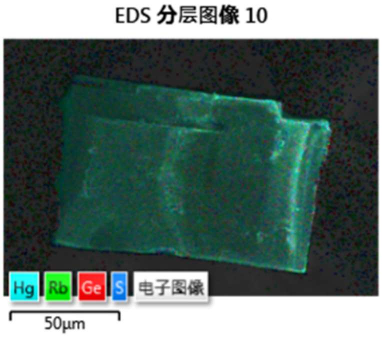

Figure S1. The element distribution images and atomic percentage (%) of $Rb_2HgGe_3S_8$.

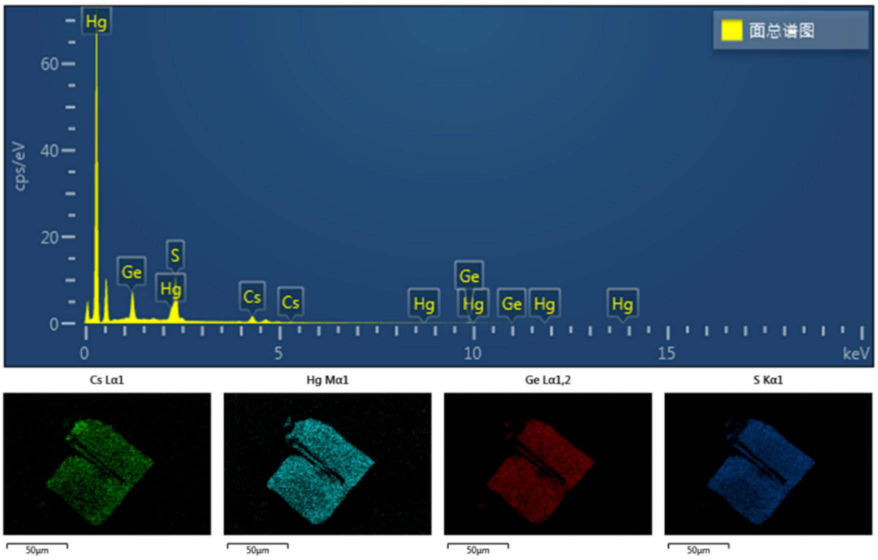

Element	Atomic percentage/%
Cs	12.06
Hg	7.99
Ge	24.82
S	55.13
Total	100

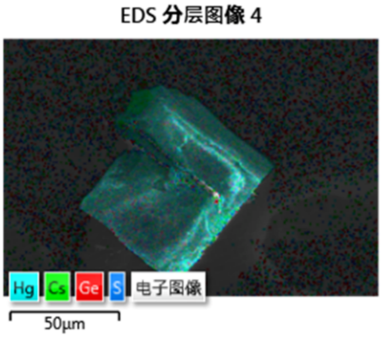

Figure S2. The element distribution images and atomic percentage (%) of $Cs_2HgGe_3S_8$

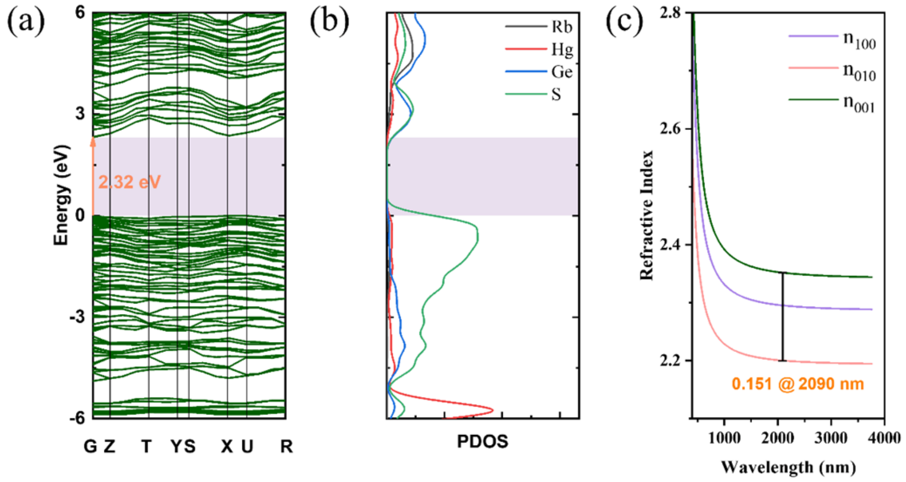

Figure S3. The calculated results of $Rb_2HgGe_3S_8$: (a) electronic band structure, (b) PDOS, (c) refractive index dispersion curve

Reference

(1) Sheldrick, G. Crystal structure refinement with SHELXL. *Acta Crystallogr., Sect. C: Struct. Chem.* 2015, *71*, 3-8.

(2) Macrae, C. F.; Sovago, I.; Cottrell, S. J.; Galek, P. T. A.; McCabe, P.; Pidcock, E.; Platings, M.; Shields, G. P.; Stevens, J. S.; Towler, M.; Wood, P. A. Mercury 4.0: from visualization to analysis, design and prediction. *J. Appl. Crystallogr.* 2020, *53*, 226-235.

(3) Simmons, E. L. Diffuse reflectance spectroscopy: a comparison of the theories. *Appl. Opt.* 1975, *14*, 1380-1386.

(4) Kurtz, S. K.; Perry, T. T. A Powder Technique for the Evaluation of Nonlinear Optical Materials. *J. Appl. Phys.* 1968, *39*, 3798-3813.

(5) Zhang, M.-J.; Jiang, X.-M.; Zhou, L.-J.; Guo, G.-C. Two phases of Ga_2S_3: promising infrared second-order nonlinear optical materials with very high laser induced damage thresholds. *J. Mater. Chem. C* 2013, *1*, 4754-4760.

(6) Clark, S. J.; Segall, M. D.; Pickard, C. J.; Hasnip, P. J.; Probert, M. J.; Refson, K.; Payne, M. C. First principles methods using CASTEP. *Zeitschrift Fur Kristallographie* 2005, *220*, 567-570.

(7) Brown, I. D.; Altermatt, D. Bond-Valence Parameters Obtained from a Systematic Analysis of the Inorganic Crystal Structure Database. *Acta Crystallographica Section B* 1985, *41*, 244-247.

(8) Ji, B.; Wang, F.; Wu, K.; Zhang, B.; Wang, J. d^6 versus d^{10}, Which Is Better for Second Harmonic Generation Susceptibility? A Case Study of $K_2TGe_3Ch_8$ (T = Fe, Cd; Ch = S, Se). *Inorg. Chem.* 2023, *62*, 574-582.